ASYMMETRIC RESPONSE OF TURBULENT CHANNEL FLOW TO WALL SUCTION AND BLOWING

Yongmann M. Chung
Mechanical Engineering Research Laboratory
Korea Electric Power Research Institute
103-16 Munji-dong, Yusong-ku, Taejon, 305-380
South Korea

Hyung Jin Sung
Department of Mechanical Engineering
Korea Advanced Institute of Science and Technology
373-1 Kusong-dong, Yusong-ku, Taejon, 305-701
South Korea

ABSTRACT

A direct numerical simulation was performed to investigate the effects of spatially-varying wall suction and blowing on turbulent channel flow. Two combinations of wall suction and blowing were considered: one is a sequence of suction and blowing (S-B) and the other is a sequence of blowing and suction (B-S). A sinusoidal form of wall suction and blowing was applied at the lower wall of the channel through a spanwise slot, downstreeam of which the flow was allowed to adjust itself to a new boundary condition at the impermeable wall. The main emphasis was placed on the asymmetric response of wall-bounded turbulent flow to different sequencies of wall suction and blowing. The rate of adjustment and the relaxations after local actuations were evaluated. It was found that the time-mean velocity and Reynolds stresses were modified significantly depending on the sequences.

INTRODUCTION

Many studies have made to delineate the effects of wall suction and blowing on wall-bounded turbulent flows (Antonia *et al.* 1995, Chung and Sung 1998). Recently, Choi, Kim and Moin (1994) applied an off-phase suction and blowing scheme to a turbulent channel flow to obtain as much as 25 % of drag reduction. It has been known that, when wall suction and blowing is actuated, there are two relaxations. One is an initial relaxation of the flow from the upstream impermeable wall boundary condition to the wall suction and blowing. The other is a back relaxation, i.e., recovery from the wall suction and blowing to the downstream impermeable wall boundary condition (Bushnell and McGinley 1989). If the slot width is long enough compared to the length scale for the initial relaxation, the flow has time enough to adjust itself to its asymptotic state corresponding to the uniform suction and blowing. On the other hand, if the slot width is shorter than the length scale for the initial relaxation, the flow cannot attain the asymptotic state. Instead, it shows a combined feature of the initial relaxation and the back relaxation, which is characterized as a growing internal layer (Alving *et al.* 1990).

In the present study, a direct numerical simulation (DNS) is performed to scrutinize the effect of spatially-varying wall suction and blowing on turbulent channel flow. A sinusoidal form of steady wall suction and blowing is applied at the lower wall of the channel through a spanwise slot which spans the whole channel width with a finite length. A schematic diagram of the model is shown in Fig. 1. Two models are considered: one is local suction first and then blowing, which is referred to as S-B hereafter, the other is B-S, *vice versa*. Downstream of the slot, the flow is allowed to adjust itself to a new boundary condition on the impermeable wall. The focus of the present paper is to investigate the asymmetric responses of wall-bounded turbulent flow to different sequencies of wall suction and blowing and to examine the evolution of downstream flow structures. The relaxations of the turbulent channel flow from the effects of these two opposite sequencies are compared.

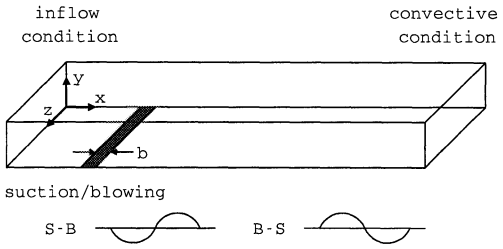

Figure 1: A schematic diagram of flow configuration.

NUMERICAL METHOD

Governing Equations

For an incompressible fluid, the unsteady three-dimensional Navier-Stokes equations can be written as :

$$\frac{\partial u_i}{\partial t} + \frac{\partial}{\partial x_j}(u_i u_j) = -\frac{\partial p}{\partial x_i} + \frac{1}{Re_m}\frac{\partial^2 u_i}{\partial x_j \partial x_j}, \qquad (1)$$

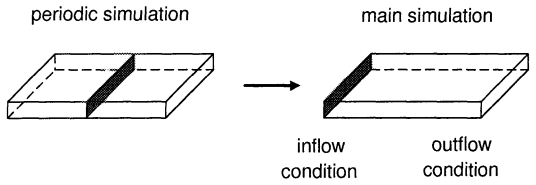

Figure 2: Inflow simulation.

where u_i is the velocity component in the x_i direction and p is the pressure. All flow variables are non-dimensionalized by the bulk mean velocity U_m and the channel half-width h. The Reynolds number is defined by $Re_m = U_m h/\nu$, where ν is the kinematic viscosity of the fluid.

A fractional-step method for solving the Navier-Stokes equations is employed (Kim Moin 1985, Yang and Ferziger 1993), which is based on a time-splitting method in conjunction with the approximate factorization technique. The solution procedure consists of a semi-implicit approach using the third-order Runge-Kutta method for the convective terms and the implicit Crank-Nicolson method for the viscous terms. For spatial discretization, second-order central differences are used on a staggered grid. The Poisson equation for p is solved in the wave number space by Fourier transformation in the streamwise (x) and spanwise (z) directions. The accuracy and reliability of the present simulation has been ascertained in the previous papers (Chung *et al.* 1997 and Chung and Sung 1997). Details regarding the numerical precedures can be found in Yang and Ferziger (1993) and Chung and Sung (1997).

To impose a real turbulence at the inflow boundary, instantaneous flow data from an auxiliary inflow simulation of a fully-developed turbulent channel flow are used with the same Reynolds number and grid spacings (Chung and Sung1997, Moin and Mahesh 1998). At the outflow boundary, the convective boundary condition used by Pauley *et al.* (1990) is employed. The periodic boundary conditions are used in the spanwise direction so that the spanwise extent of the slot is assumed to be infinite. The no-slip conditions are used on the channel walls. The wall-normal velocity (v_w) is imposed at the slot in the lower wall, making other components of the velocity (u, w) zero.

$$v_w = \begin{cases} A(x-6)(x-8), & 6 \le x \le 8, \\ -A(x-8)(x-10), & 8 \le x \le 10. \end{cases} \quad (2)$$

Here, A represents the strength of the wall suction and blowing. $A > 0$ means suction in the first half of the slot followed by blowing in the second half, which is the case of S-B. $A < 0$ means the opposite one for B-S. All the computations are performed on a CRAY-YMP-C90 at the Supercomputer Center of Electronics and Telecommunications Research Institute (ETRI).

RESULTS AND DISCUSSION

Numerical Parameters

	grid points	L_x	Δ_x
Case 1	$256 \times 97 \times 96$	25.6	10.0
Case 2	$256 \times 97 \times 96$	32.0	12.5
Case 3	$256 \times 97 \times 96$	51.2	20.0

Table 1: Numerical parameters used in the grid refinement

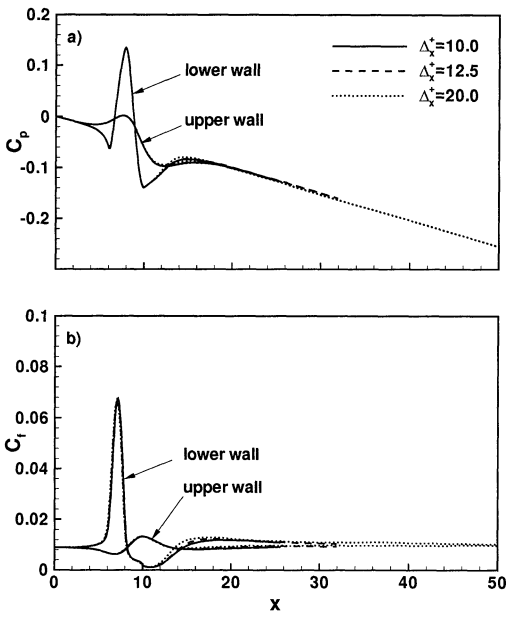

Figure 3: Validation of grid resolution with a) pressure coefficient C_p and b) skin friction coefficeint C_f.

In the present study, an incompressible turbulent channel flow between two parallel plates is considered. A configuration of the flow and relevant coordinate definitions are illustrated in Fig. 1. The Reynolds number is $Re_m = 1500$, which corresponds to $Re_\tau = 100$.

Streamwise and spanwise dimensions of the computational domain are set $L_x = 24h$ and $L_z = 4h$, respectively. With the present grid system ($256 \times 97 \times 64$) in the x, y, z directions, the streamwise and spanwise grid resolutions are $\Delta x^+ = 10.0$ and $\Delta z^+ = 6.25$, respectively. The time step is $\Delta t = 0.02h/U_m$, i.e., $\Delta t^+ = 0.14$ in wall units. After a transient period, converged time-mean quantities are obtained for $10,000\Delta t$, which corresponds to $T = 200h/U_m$.

As shown in Fig. 1, a sequence of steady suction and blowing is imposed through the spanwise slot located at the lower wall. The width (or downstream extent) of the slot is $b^+ = 400$ in wall units. The slot begins at $x = 6$ and the downstream edge of the slot is located at $x = 10$. In the case of S-B, suction is applied at the first half of the slot from $x = 6$ to $x = 8$ and blowing is at the second half from $x = 8$ to $x = 10$. For B-S, the order of suction and blowing is reversed. Accordingly, the net mass flux into the flow field through the slot is zero.

As an inflow simulation, a fully-developed turbulent channel flow is performed. The main advantage of this inflow condition is that it can provide a turbulence inflow with correct phase information and dynamics, although the inflow simulation requires additional computation time and data storage. As sketched in Fig. 2, the instantaneous velocity field from the inflow simulation on a plane perpendicular to the streamwise direction is stored at each time step (Chung and Sung1997). The data is then replaced at the inlet plane of the main simulation to specify the inflow condition. The periodic boundary conditions are used in the streamwise and spanwise directions assuming that the flow is homogeneous in those directions. The streamwise and spanwise dimensions of the inflow simulation are $12.8h$ and $4h$, respectively. A $128 \times 97 \times 64$ grid system is used and the grid spacings are the same as in the main simulation.

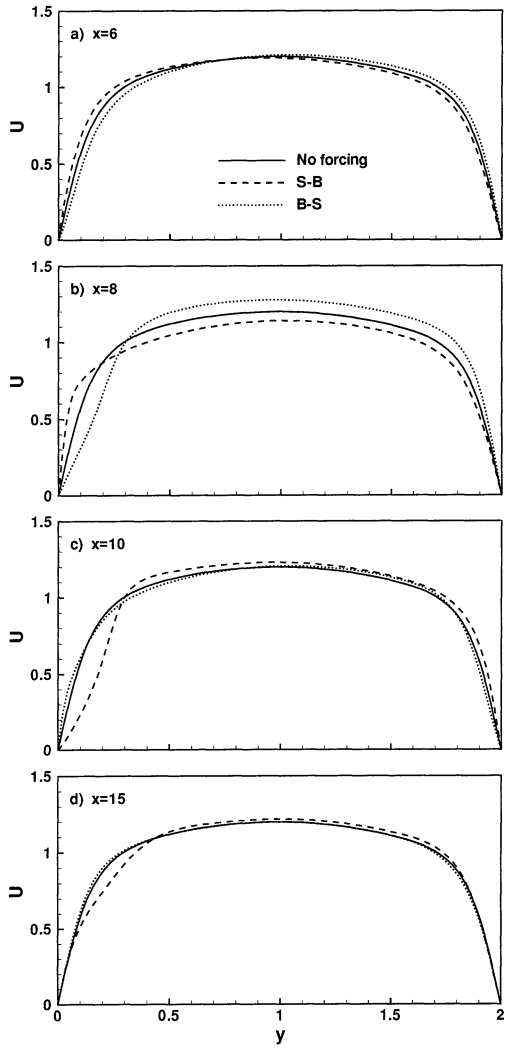

Figure 4: Variations of U at several downstream locations.

Grid Refinement

Grid refinements are performed to ensure that the grid resolutions used in this study are adequate to reslove the downstream evolution of turbulent channel flow with wall suction and blowing. In turbulent channel flow, the dominant flow structures are the streamwise vortices near the wall. The average streamwise length of the streamwise vortices is $\lambda_x^+ \approx 1000$ (Blackwelder and Eckelmann 1979) in wall units while the average spanwise spacing is $\lambda_z^+ \approx 100$ (Kline *et al.* 1967) regardless of the Reynolds number. Geometric characteristics of the streamwise vortices reveal that much finer grid spacing is needed in the spanwise direction compared to the streamwise direction. Due to the wall proximity of the streamwise vortices, grid clustering is implemented near the channel wall.

As wall suction and blowing is applied, the streamwise vortices move up and down. When the streamwise vortices move away from the wall due to the wall blowing, a finer grid in the core region is necessary to resolve the streamwise vortices, while when it moves to the wall, much finer grid resolution is needed for the shrinked streamwise

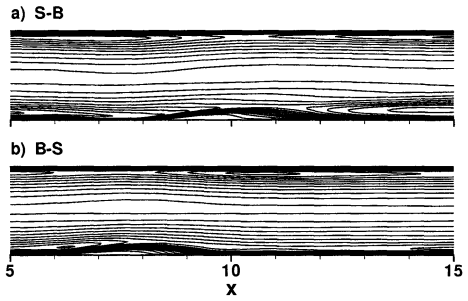

Figure 5: Contours of u'/u_τ. a) S-B, b) B-S.

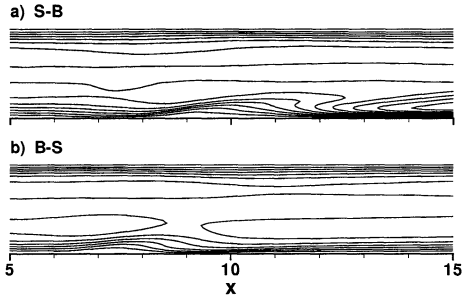

Figure 6: Contours of v'/u_τ. a) S-B, b) B-S.

vortices located very close to the wall.

To examine the grid resolutions in the streamwise direction, a preliminary simulation of turbulent channel flow with wall suction and blowing is performed with three different streamwise resolutions. The numerical parameters used in this test are listed in Table 1. The same inflow condition from an inflow simulation is employed to exclude the effect of inflow condition. The wall pressure coefficient C_p and the skin-friction coefficient C_f at the lower and upper walls show a good convergence for all three resolutions throughout the domain as shown in Fig. 3.

Time-mean velocity

Effects of the spatially-varying wall suction and blowing on time-mean streamwise velocity (U) are evaluated in Fig. 4. Wall blowing reduces the streamwise velocity near the lower wall by the injection of low momentum fluid while the momentum flux is slightly increased in the upper wall due to the continuity constraint within the channel. Accordingly, the velocity profiles are distorted and asymmetric to the channel centerline. When wall suction is applied, opposite phenomena are observed: the velocity near the lower wall increases due to the suction of low momentum fluid, whereas the velocity near the upper wall decreases slightly. As the flow passes the slot, the flow field adjusts itself from the direct influence of wall suction and blowing ($x = 10$). The recovery of time-mean velocity begins from the near-wall region. In the case of S-B, the low momentum fluid region caused by the blowing propagates to the channel core region, while the velocity profiles for B-S approach the unperturbed channel profiles.

Turbulence statistics

Contours of the Reynolds normal stresses (u', v', w') and the Reynolds shear stress $(-\overline{u'v'})$ in the $x - y$ plane are shown in Figs. 5, 6, 7 and 8. Since wall suction and blowing is enforced in the lower wall, the effect is more significant in the lower part of the channel than in the upper part. In

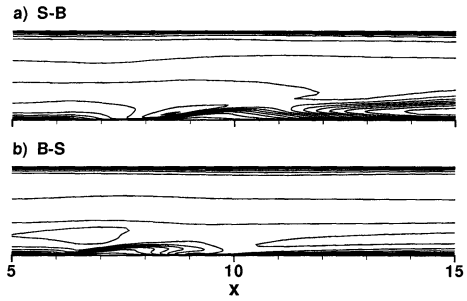

Figure 7: Contours of w'/u_τ. a) S-B, b) B-S.

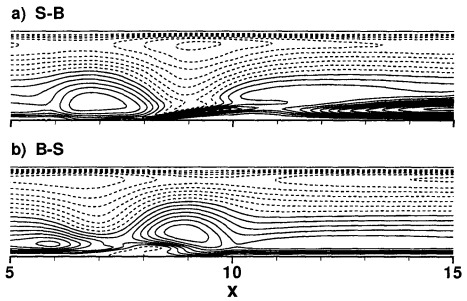

Figure 8: Contours of $-\overline{u'v'}/{u_\tau}^2$. a) S-B, b) B-S.

the case of S-B, the contour lines first bend toward the slot due to wall suction with a reduced magnitude, and then move to the core by wall blowing, and finally become parallel to the wall as the flow passes the slot. In the case of B-S, on the contrary, the contour lines first move upward due to wall blowing and then move to the lower wall by suction. When blowing is applied in both cases, an internal layer emanating from the upstream edge of the blowing slot appears and it moves away from the wall. It is shown that the Reynolds normal stress inside the internal layer is negligible. In the S-B case, when the no-slip boundary condition is imposed following the blowing, another internal layer evolves as the flow begins to adjust itself to the no-slip condition. As the flow goes further downstream, the interaction of two internal layers gives rise to a stress bore, i.e., a region of elevated stress which moves away from the wall. On the other hand, in the B-S case, the region of low stress induced by blowing is confined to a small area. These features are observed in all three components of the Reynolds normal stess and shear stress.

In order to look into the detailed influences of wall suction and blowing, profiles of the normal components of the Reynolds stress (u', v' and w') are displayed in Fig. 9. All the components are normalized by the friction velocity u_τ calculated at inlet. At $x = 6$, upsteam edge of the slot, the turbulence intensities in the lower half part decrease in the S-B case, while the intensities increase in the B-S case, showing a small upstream effect of the wall suction and blowing. At $x = 8$, the streamwise (u') and spanwise (w') turbulence intensities change substantially in the lower half part of the channel.

For the second half of the slot ($8 < x < 10$), opposite features are detected as the wall boundary conditions are reversed for both cases. When blowing is applied, the location of the peak value moves away from the lower wall, while the peak is located close to the lower wall with suction. The degree of outward (inward) shift is proportional to the accumulated amount of suction and blowing. The outward (inward) shift of u' is linked to the outward (inward) movement of the streamwise vortices, which is consistent with the findings in the boundary layer flow by Choi *et al.* (1997).

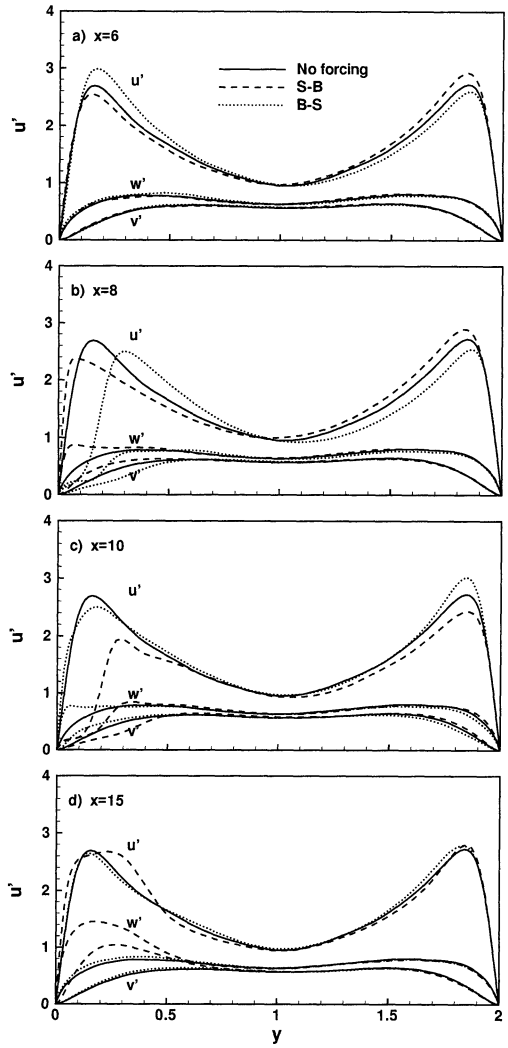

Figure 9: Variations of u'/u_τ, v'/u_τ, and w'/u_τ.

As the flow evolves downstream, variations of the profiles for S-B become appreciable due to the accumulated effect of suction and blowing while the profiles for B-S are similar to those of no forcing. The relaxation process of S-B is dominated by the internal layer emanating from the downstream edge of the slot as the flow adjusts itself to the no-slip condition. Turbulent intensities begin to recover in the vicinity of the lower wall, as the internal layer evolves. The profiles of u' have two peaks: one obtained from the internal layer, the other from the upstream turbulent flow. The inner peak obtained from the internal layer moves closer to the lower wall than in the unperturbed channel flow, while the outer peak moves slowly to the core region. At $x = 15$, there is a region of elevated stress moving away from the wall with increasing the downstream distance. The stress bore was also observed in the boundary layer over convex curvature by Alving, Smits & Watmuff (1990).

Instantaneous vorticity field

Contours of the streamwise vorticity ω_x in the $y-z$ plane

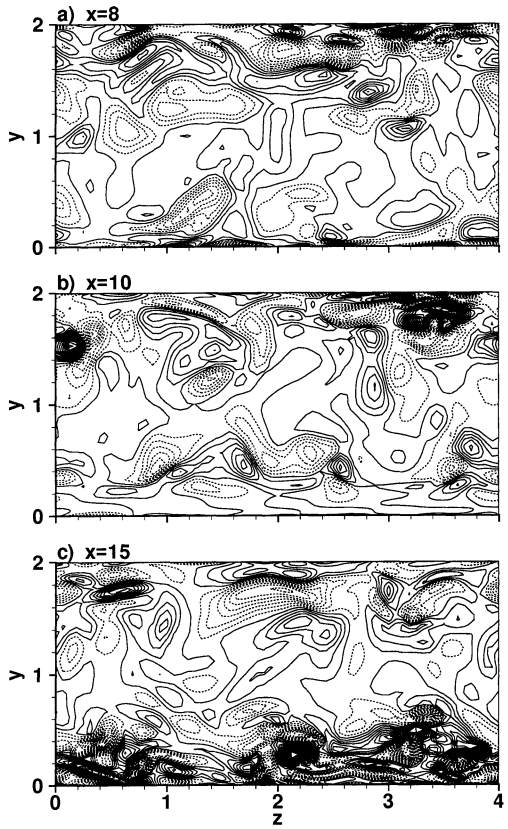

Figure 10: Variations of ω_x for S-B.

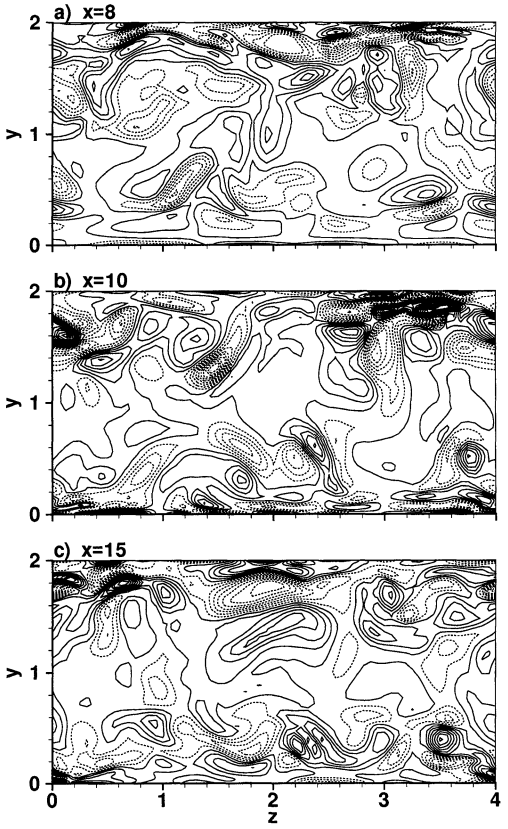

Figure 11: Variations of ω_x for B-S.

are shown in Figs. 10 and 11 for two cases, respectively. The vortical structures are mainly confined to the near-wall region of the channel flow in the upstream of the slot. As wall suction is applied, vortices move down to the lower wall, while vortices are lifted into the core with blowing. In the case of S-B, vortices in the lower half of the channel first move down to the wall in the first half of the slot ($6 \leq x \leq 8$), and then they are lifted away from the lower wall in the second half ($8 \leq x \leq 10$). On the other hand, the vortices for B-S are first lifted into the core ($6 \leq x \leq 8$), and then they move down to the lower wall ($8 \leq x \leq 10$).

As the vortices move away from the wall due to blowing, a region of negligible vorticities appears near the lower wall. At the downstream edge of the slot ($x = 10$), the vortices for the S-B case are located quite above the lower wall to a considerable strength. Unlike the S-B case, the streamwise vortices for the B-S case remain in the original position. It is seen that the wall suction and blowing in the case of B-S acts like a streamlined obstacle and the flow passes by the obstacle smoothly.

Downstream evolution

Downstream variations of the Reynolds stress are shown in Fig. 12 for both cases. To examine the different responses to wall suction and blowing, each component of the Reynolds stress is plotted. E_i represents the whole turbulent kinetic energy in the x_i direction, which is normalized by its inflow value. The definition of E_i is given as,

$$E_i(x) = \frac{\int_0^{2h} u_i'(x,y)dy}{\int_0^{2h} u_i'(0,y)dy}. \quad (3)$$

S-B has a prolonged influence on the downstream evolution of turbulent channel flow while the effect of B-S is confined to a short downstream distance near the slot. In the case of S-B, the response of u' is faster than two other components of the Reynolds stress. As suction is applied at $x = 6$, u' begins to increase, and then it decreases to a minimum at the downstream end of the slot ($x = 10$). The minimum value of u' is much lower than that in the unperturbed channel. This is mainly attributed to the reduction in the lower half of the channel as shown in Fig. 9(c) . The responses of v' and w' are slightly delayed and they also have a minimum. Downstream of the slot, all components of the Reynolds stress increase until they have a maximum. The increase of v' and w' is much larger than that of u', which is also consistent to Fig. 9.

Unsteady flow field

Contour plots of the instantaneous streamwise velocity (u') are demonstrated for two cases. Due to the low momentum fluid ejected from the blowing slot, near-wall structures are lifted-up, resulting in the discontinuity of the low-speed streaks in Fig. 13 (a). It appears that the low-speed streaks are not destroyed but just lifted away from the lower wall. It is known that wall blowing activates the turbulence motion while suction diminishes it (Sumitani and Kasagi 1995). This features are related to the streamwise vortices located near the wall. In the case of S-B, the turbulence motions downstream of the slot become more energetic due to the lifted streamwise vortices. On the contrary, the turbulence motion downstream the slot for B-S is similar to that upstream of the slot.

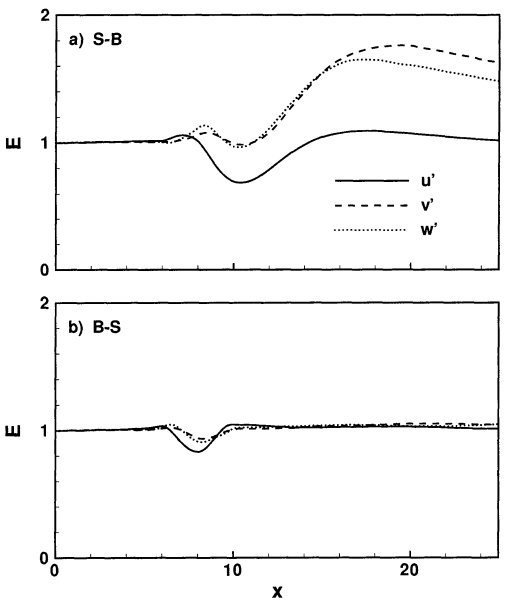

Figure 12: Downstream variations of turbulent kinetic energy. a) S-B and b) B-S.

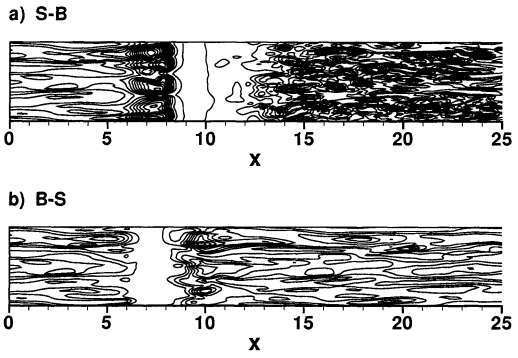

Figure 13: Instantaneous velocity contours of u near the lower wall. a) S-B, b) B-S.

CONCLUDING REMARKS

The responses of turbulent channel flow to spatially-varying wall suction and blowing has been investigated by direct numerical simulation. Two sequences of wall suction and blowing were considered: one is suction followed by blowing (S-B) and the other is blowing followed by suction (B-S). Wall suction and blowing was imposed at the lower wall of the channel flow through a spanwise slot. When blowing was applied, an internal layer emanating from the upstream edge of the blowing slot appeared and it moved away from the wall. In the S-B case, another internal layer evolved as the flow began to adjust itself to the no-slip condition following the blowing. The interaction of two internal layers gived rise to a stress bore, i.e., a region of elevated stress which moved away from the wall. In the B-S case, on the other hand, the internal layer induced by blowing is confined to a small area. Consequently, the downstream evolution of turbulent flow following the wall suction and blowing was substantially different for two sequences. S-B had a prolonged influence on the downstream evolution of turbulent flow while the effect of B-S was confined to a small downstream distance near the slot. The turbulent flow recovering from the sequence of S-B was found to have a sustained higher skin friction level than in that recovering from the sequence of B-S. Three components of Reynolds stress were amplified by S-B but with different degrees. The recovery process of each component of Reynolds stress was different from each other.

ACKNOWLEDGEMENT

The authors appreciate Prof. K. S. Yang at Inha University for his helpful comments and suggestions.

REFERENCES

Alving, A. E., Smits, A. J. and Watmuff, J. H., 1990, "Turbulent boundary layer relaxation from convex curvature," *Journal of Fluid Mechanics*, Vol. 211, pp. 529–556.

Antonia, R. A., Zhu, Y., and Sokolov, M., 1995, "Effect of concentrated wall suction on a turbulent boundary layer," *Physics of Fluids*, Vol. 7, No. 10, pp. 2465–2474.

Blackwelder, R. F., and Eckelmann, H., 1979, "Streamwise vortices associated with the bursting phenomenon," *Journal of Fluid Mechanics*, Vol. 94, pp. 577–594.

Bushnell, D. M., and McGinley, C. B., 1989. "Turbulence control in wall flows," *Annual Review of Fluid Mechanics*, Vol. 11, pp. 1–20 .

Choi, H., Moin, P., and Kim, J., 1994, "Active turbulent control for drag reduction in wall-bounded flows," *Journal of Fluid Mechanics*, Vol. 262, pp. 75–110.

Choi, H., Park, J., and Hahn, S., 1997, "Effects of blowing/suction from a spanwise slot on a turbulent boundary layer flow," In *Eleventh Symposium on the Turbulent Shear Flows*, Grenoble, France, September 8-10, 1997. pp. P1-37–P1-42.

Chung, Y. M., and Sung, H. J., 1997, "Comparative Study of Inflow Conditions for Spatially Evolving Simulation," *AIAA Journal*, Vol. 35, No. 2, pp. 269–274.

Chung, Y. M., and Sung, H. J., 1998, " Effects of local blowing on spatially-evolving turbulent channel flow," In *Proceedings of The Fourth KSME-JSME Fluids Engineering Conference*, pp. 673–676.

Chung, Y. M., Sung, H. J., and Boiko, A. V., 1997, "Spatial simulation of the instability of channel flow with local suction/blowing," *Physics of Fluids*, Vol. 9, No. 11, pp. 3258–3266.

Kim, J., and Moin, P., 1985, "Application of a fractional-step method to incompressible Navier-Stokes equations," *Journal of Computational Physics*, Vol. 59, pp. 308–323.

Kline, S. J., Reynolds, W. C., Schraub, F. A., and Runstadler, P. W., 1967, "The structure of turbulent boundary layers," *Journal of Fluid Mechanics*, Vol. 30, pp. 741–773.

Moin, P., and Mahesh, K., 1998, "Direct numerical simulation: A tool in turbulence research," *Annual Review of Fluid Mechanics*, Vol. 30, pp. 539–578.

Pauley, L. R., Moin, P., and Reynolds, W. C., 1990, "The structure of two-dimensional separation," *Journal of Fluid Mechanics*, Vol. 220, pp. 397–411.

Sumitani, Y., and Kasagi, N., 1995, "Direct numerical simulation of turbulent transport with uniform wall injection and suction," *AIAA Journal*, Vol. 33, No. 7, pp. 1220–1228.

Tardu, S., "Near wall turbulence control by local time periodical blowing," *Experimental Thermal and Fluid Science*, Vol. 16, pp. 41–53.

Yang, K. S., and Ferziger, J. H., 1993, "Large-eddy simulation of turbulent obstacle flow using a dynamic subgrid-scale model," *AIAA Journal*, Vol. 31, No. 8, pp. 1406–1413.